Contribution from the Department of Chemistry,
Tulane University, New Orleans, Louisiana 70118

Independent Control of Charge-Transfer and Metal-Centered Excited States in Mixed-Ligand Polypyridine Ruthenium(II) Complexes via Specific Ligand Design

William F. Wacholtz, Roy A. Auerbach,* and Russell H. Schmehl*

Received April 1, 1985

A series of tris(polypyridine)ruthenium(II) complexes $[Ru(dmb)_3]^{2+}$, $[Ru(dmb)_2(decb)]^{2+}$, $[Ru(dmb)(decb)_2]^{2+}$, and $[Ru(decb)_3]^{2+}$ have been prepared, where dmb is 4,4′-dimethyl-2,2′-bipyridine and decb is 4,4′-bis(ethylcarboxy)-2,2′-bipyridine. Absorption and emission energies decrease in the order $[Ru(dmb)_3]^{2+} > [Ru(decb)_3]^{2+} > [Ru(dmb)(decb)_2]^{2+} > [Ru(dmb)_2(decb)]^{2+}$ and are linearly related to $\Delta E°$, the difference between the first oxidation and reduction potentials of the complex. Temperature-dependent emission quantum yields and lifetimes in CH_2Cl_2 yield activation barriers, $\Delta E'$, for nonradiative decay from the ^{3}MLCT state. For $[Ru(dmb)_3]^{2+}$ and $[Ru(decb)_3]^{2+}$ the $\Delta E'$ values are 2750 and 1180 cm^{-1}, respectively, and represent the thermal barrier to population of a metal-centered excited state. Upon photolysis in the presence of Cl^- in CH_2Cl_2, substitution occurs, resulting in the cis chloro complex. The mixed-ligand complexes exhibit much smaller activation barriers for nonradiative decay and do not undergo anation upon prolonged photolysis in the presence of Cl^-. The nonradiative decay and photosubstitution results are discussed in terms of the energetic separation between the ^{3}MLCT and ^{3}MC states.

Introduction

The photochemistry of transition-metal complexes having metal to ligand charge-transfer (MLCT) transitions as the lowest energy excited state has been a topic of great interest in inorganic photochemistry.[1] The focus of much research in this area has involved an examination of the relationship between the MLCT energies of a series of complexes and the photochemical lability of the systems;[2] data available suggest photosubstitution results from population of low-energy ligand field states that are not spectroscopically observed. For series of complexes that have been examined, such as $[Ru(NH_3)_5(pyX)]^{2+}$, $[Fe(CN)_5(pyX)]^{3-}$, and $[Re(\eta^5\text{-}C_5H_5)(CO)_2(pyX)]$,[3-5] where pyX is a series of substituted pyridines, the quantum yield for ligand loss decreases as substituents are added that decrease the energy of the MLCT state. The decrease in the substitution yield occurs as the MLCT state becomes isolated from communication with the ligand field states responsible for photosubstitution.

The photophysical and photochemical properties of numerous ruthenium(II) and osmium(II) polypyridyl complexes have been thoroughly examined. For ruthenium, the MLCT state exhibits emission in the red that allows the characterization of the decay. Scheme I outlines the photophysical decay pathways common to many ruthenium bipyridyl complexes. Excitation is followed by rapid intersystem crossing from the initially formed ^{1}MLCT to a ^{3}MLCT state[6,7] and is believed to occur with nearly unit efficiency for $[Ru(bpy)_3]^{2+}$.[8] The triplet charge-transfer state decays via both temperature-dependent and temperature-independent processes[9-14] and the thermally activated decay mode has been

Scheme I

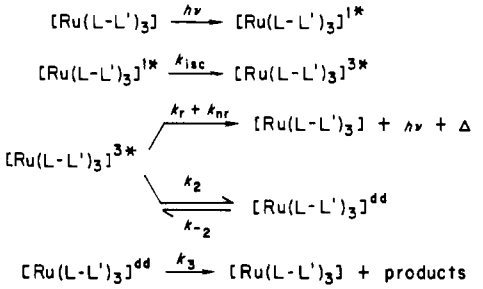

ascribed to internal conversion to a triplet metal-centered state, ^{3}MC. In nonpolar aprotic solvents the ruthenium complexes undergo efficient photoanation, and the photoreactivity appears to occur via population of the ^{3}MC state.[9,13,15-19] If the photolabile state is indeed metal-centered, and this state is populated principally by internal conversion from the ^{3}MLCT, it should be possible to design complexes that are inert to photosubstitution. The energy of the ^{3}MC state will be influenced principally by the σ-donating strength of the ligands and the MLCT state energy depends principally on the energy of the lowest ligand π^* orbitals. Preparation of complexes having one bipyridine with a low-energy π^* level and more basic bipyridines filling the remaining coordination sites may result in ruthenium polypyridine complexes having ^{3}MC states thermally inaccessible from the ^{3}MLCT. Since most polypyridyl complexes of ruthenium(II) luminesce in fluid solution at room temperature, it is possible to monitor the ^{3}MLCT to ^{3}MC internal conversion as a function of systematic structural variations associated with the ligands.

Very recently several groups have presented results of photophysical studies of several ruthenium polypyridyl complexes that suggest such separation of ^{3}MLCT and ^{3}ML states. In examining mixed-ligand complexes containing both bpy and 2,2′-biquinoline,[14] Barigelletti and co-workers have observed only a slight temperature dependence of luminescence lifetimes between 77 K and room temperature. Such an observation is expected when thermal activation to a ^{3}MC state is no longer feasible energetically.

(1) See for example: (a) "Inorganic and Organometallic Photochemistry"; Wrighton, M. S., Ed.; American Chemical Society: Washington, DC, 1978; Adv. Chem. Ser. No. 168. (b) Whitten, D. G. *Acc. Chem. Res.* **1980**, *13*, 83. (c) Meyer, T. J. *Prog. Inorg. Chem.* **1983**, *39*, 389. (d) Seddon, K. R. *Coord. Chem. Rev.* **1982**, *41*, 79. (e) Balzani, V.; Boletta, F.; Gandolfi, M. T.; Maestri, M. *Top. Curr. Chem.* **1978**, *71*, 1.
(2) For two recent reviews see: (a) Ford, P. C.; Wink, D.; Dibenedetto, J. *Prog. Inorg. Chem.* **1983**, *30*, 213. (b) Ford, P. C. *Rev. Chem. Intermed.* **1978**, *2*, 267.
(3) Malouf, G.; Ford, P. C. *J. Am. Chem. Soc.* **1977**, *99*, 7213.
(4) Figard, J. E.; Petersen, J. D. *Inorg. Chem.* **1978**, *17*, 1059.
(5) Giordano, P. J.; Wrighton, M. S. *Inorg. Chem.* **1977**, *16*, 160.
(6) (a) Porter, G. B.; Schlafer, H. L. *Ber. Bunsenges. Phys. Chem.* **1964**, *68*, 316. (b) Crosby, G. A.; Perkins, W. G.; Klassen, D. M. *J. Chem. Phys.* **1965**, *43*, 1498. (c) Lytle, F. E.; Hercules, D. M. *J. Am. Chem. Soc.* **1969**, *91*, 253.
(7) (a) Harrigan, R. W.; Crosby, G. A. *J. Chem. Phys.* **1973**, *59*, 3468. (b) Hipps, K. W.; Crosby, G. A. *J. Am. Chem. Soc.* **1975**, *97*, 7042. (c) Crosby, G. A. *Acc. Chem. Res.* **1975**, *8*, 231 and references therein. (d) Felix, F.; Ferguson, J.; Gudel, H. C.; Ludi, A. *J. Am. Chem. Soc.* **1980**, *102*, 4096.
(8) (a) Boletta, F.; Juris, A.; Maestri, M.; Sandrini, D. *Inorg. Chem. Acta* **1980**, *44*, L175. (b) Demas, J. N.; Taylor, D. G. *Inorg. Chem.* **1979**, *18*, 3177.
(9) (a) Van Houten, J.; Watts, R. J. *Inorg. Chem.* **1978**, *17*, 3381. (b) Van Houten, J.; Watts, R. J. *J. Am. Chem. Soc.* **1976**, *98*, 4853.
(10) Allsopp, S. R.; Cox, A.; Kemp, T. J.; Reed, W. J. *J. Chem. Soc., Faraday Trans. 1* **1978**, 1275.
(11) Cherry, W. R.; Henderson, L. J. *Inorg. Chem.* **1984**, *23*, 983.
(12) (a) Caspar, J. V.; Sullivan, B. P.; Kober, E. M.; Meyer, T. J. *Chem. Phys. Lett.* **1982**, *91*, 91. (b) Caspar, J. V.; Meyer, T. J. *Inorg. Chem.* **1983**, *22*, 2444. (c) Caspar, J. V.; Meyer, T. J. *J. Am. Chem. Soc.* **1983**, *105*, 5583.
(13) Durham, B.; Caspar, J. V.; Nagle, J. K.; Meyer, T. J. *J. Am. Chem. Soc.* **1982**, *104*, 4803.
(14) Barigelletti, F.; Juris, A.; Balzani, V.; Belser, P.; Zelewsky, A. V. *Inorg. Chem.* **1983**, *22*, 3335.
(15) Fasano, R.; Hoggard, P. E. *Inorg. Chem.* **1983**, *22*, 567.
(16) Jones, R. F.; Cole-Hamilton, D. J. *Inorg. Chim. Acta* **1981**, *53*, L3.
(17) Allen, G. H.; White, R. P.; Rillema, D. P.; Meyer, T. J. *J. Am. Chem. Soc.* **1984**, *106*, 2613.
(18) Crutchley, R. J.; Lever, A. B. P. *Inorg. Chem.* **1982**, *21*, 2276.
(19) Pinnick, D. V.; Durham, B. *Inorg. Chem.* **1984**, *23*, 1440.

0020-1669/86/1325-0227$01.50/0

Table I. Redox Properties of Complexes Examined[a]

complex	oxidn	reductions			
	$E°(3+/2+)$, V	$E°(2+/+)$, V	$E°(+/0)$, V	$E°(0/-)$, V	$\Delta E°$,[b] V
$[Ru(dmb)_3]^{2+}$	1.10	−1.46	−1.63	−1.86	2.56
$[Ru(dmb)_2(decb)]^{2+}$	1.30	−1.03[5]	−1.53	−1.72[5]	2.33
$[Ru(dmb)(decb)_2]^{2+}$	1.44	−0.96[5]	−1.16	−1.64	2.40
$[Ru(decb)_3]^{2+}$	1.55	−0.91	−1.05	−1.27	2.46
$[Ru(bpy)_3]^{2+}$	1.28	−1.32	−1.52		2.60

[a] Potentials vs. SSCE reference in CH_3CN with tetrabutylammonium hexafluorophosphate as supporting electrolyte; v = 200 mV/s. [b] Potential difference between the first oxidation and first reduction.

Results of this type have also been made by Cherry, examining temperature-dependent luminescence in water of mixed-ligand complexes of Ru(II) having both bpy and 4,4′-dicarboxy-2,2′-bipyridine.[11] Further, Meyer and co-workers have thoroughly examined complexes having bpy and either bipyrazine, bipyrimidine, or 4,4′-dicarbamoyl-2,2′-bipyridine.[17,20]

We report here the examination of a series of mixed bipyridyl complexes of ruthenium(II) having 4,4′-dimethyl-2,2′-bipyridine (dmb) and 4,4′-bis(ethylcarboxy)-2,2′-bipyridine (decb) as ligands.

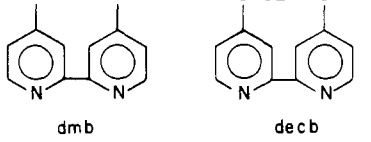

dmb decb

The complexes prepared are $[Ru(dmb)_3]^{2+}$ (**1**), $[Ru(dmb)_2(decb)]^{2+}$ (**2**), $[Ru(decb)_2(dmb)]^{2+}$ (**3**), and $[Ru(decb)_3]^{2+}$ (**4**). In this work the energetic relation between ground and charge-transfer states for this series is described on the basis of the electrochemical and spectroscopic properties of the complexes. Temperature-dependent emission quantum yields and luminescence lifetimes are also reported; activation barriers obtained are related to normal-region electron transfer between the ^{3}MLCT and ^{3}MC states.[1c] The temperature-dependent photosubstitution of complexes **1** and **4** by Cl^- in CH_2Cl_2 has also been examined. Results are discussed in terms of the energetic relationship between the ^{3}MLCT and ^{3}MC states, relating $\Delta E'$, the activation barrier for internal conversion between the states, to the nature of the equilibrium of the process.

Results

Electrochemistry. The $E°$ values for the complexes, determined by cyclic voltammetry, are listed in Table I. The redox behavior for both oxidation and reduction of all four complexes indicates electrochemical reversibility (ΔE_p = 60–80 mV) and chemical stability of the redox products ($i_{p,a}/i_{p,c}$ = 1) on the time scale of the experiment. Sequential replacement of the dmb ligands of **1** with decb results in increases in the $Ru^{3+/2+}$ potential, from 1.10 V for **1** to 1.55 V for **4**. Similar results have been obtained by Rillema et al. for related mixed ligand complexes.[21] Reduction of ruthenium bipyridyl complexes has been shown to be ligand-localized on the basis of UV–vis[22] and ESR[23] spectra. In these complexes, the first reduction is observed at −1.46 V for **1** and at −0.91 V for **4**. The mixed-ligand derivatives, **2** and **3**, both exhibit first reductions indicating reduction of coordinated decb. The second reduction of **3** occurs at −1.16 V compared to −1.53 V for **2**, reflecting differences in the nature of the second reducible ligand in the two complexes. The potentials for reduction of $[Ru(decb)_3]$ agree well with those reported by Elliott.[22]

Absorption and Emission Spectra. The absorption spectra of all of the complexes exhibit UV transitions corresponding to intraligand $\pi \rightarrow \pi^*$ transitions between 290 and 310 nm (Table II). For complexes **1** and **4**, a single maximum in the 400–500-nm region is observed (Figure 1) and has been assigned as a metal to ligand charge-transfer (MLCT) transition.[6,7c] The complexes having both of the bipyridine ligands, **2** and **3**, exhibit two maxima between 400 and 500 nm, indicative of two independent MLCT transitions. Here, the lowest energy MLCT maximum of both **2** and **3** is red-shifted relative to that of **4**. The red shift in the $d \rightarrow \pi^*$ transition is related to both the reduction in symmetry of the mixed-ligand complexes as well as the cumulative inductive effect of the σ-donating and π-withdrawing ligand orbitals.

Room-temperature emission spectra of **1**–**4**, corrected for photomultiplier response, are shown in Figure 2. Emission maxima in CH_2Cl_2 at room temperature and 77 K are listed in Table II. Relative energies of absorption and emission maxima for **1**–**4** and values of $\Delta E°$, the potential difference between the first oxidation and first reduction for the complexes (Table I), have the same ordering: **1** > **4** > **3** > **2**. The result indicates that

Table II. Absorption and Emission Maxima of Ruthenium(II) Polypyridyl Complexes in Methylene Chloride

complex	abs max,[a] cm^{-1}			emissn max,[b] cm^{-1}	
	$\pi \rightarrow \pi^*$	$d \rightarrow \pi_1^*$	$d \rightarrow \pi_2^*$	298 K	77 K
$[Ru(bpy)_3]^{2+}$	34 500	22 100		16 560	17 200
$[Ru(dmb)_3]^{2+}$	34 700	21 800		16 180	16 850
$[Ru(dmb)_2(decb)]^{2+}$	35 000	20 300	23 300	14 390	15 580
$[Ru(dmb)(decb)_2]^{2+}$	32 500	20 700	22 600	15 200	15 830
$[Ru(decb)_3]^{2+}$	32 500	21 413		15 900	16 480

[a] Maxima ±100 cm^{-1}. [b] Maxima ±50 cm^{-1}.

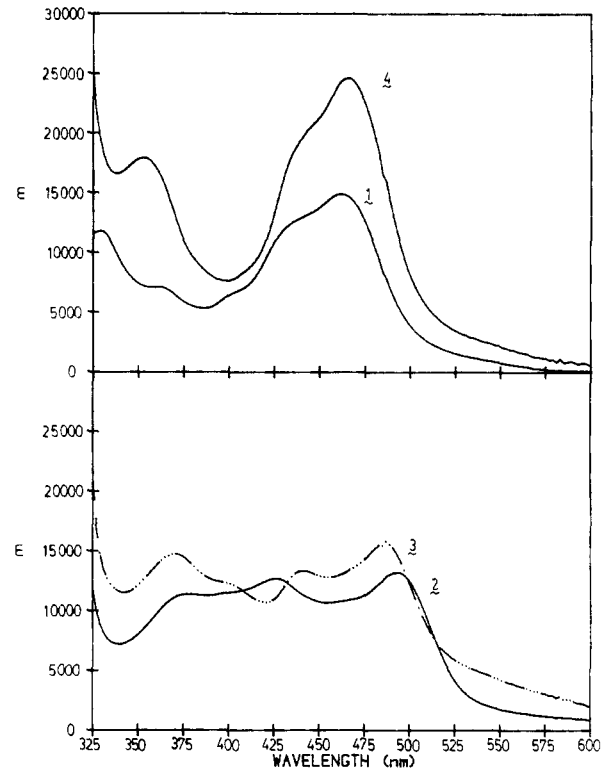

Figure 1. Visible absorption spectra in CH_2Cl_2 for $[Ru(dmb)_3]^{2+}$ (**1**), $[Ru(decb)_3]^{2+}$ (**4**), $[Ru(dmb)_2(decb)]^{2+}$ (**2**) and $[Ru(decb)_2(dmb)]^{2+}$ (**3**).

(20) Neveux, P. E.; Meyer, T. J., private communication.
(21) Rillema, D. P.; Allen, G.; Meyer, T. J.; Conrad, D. *Inorg. Chem.* **1983**, *22*, 1617.
(22) Elliot, C. M.; Hershenhart, E. J. *J. Am. Chem. Soc.* **1982**, 104, 7519.
(23) DeArmond, M. K.; Carlin, C. M. *Coord. Chem. Rev.* **1981**, *36*, 325.
(24) Klassen, D. M. *Chem. Phys. Lett.* **1982**, *93*, 383.

Table III. Activation Parameters for the Decay of the ^{3}MLCT State from Temperature-Dependent Emission Quantum Yields and Lifetimes[a]

	ϕ_{em}				τ		
complex	$\Delta E'$, cm^{-1}	k_0', s^{-1}	$10^{-5}k_1$, s^{-1}	$10^{-5}\eta_{isc}k_r$, s^{-1}	$\Delta E'$, cm^{-1}	k_0', s^{-1}	$10^{-5}k_1$, s^{-1}
$Ru(bpy)_3^{2+}$ [b]	3070 ± 250	4 ± 2 × 10^{12}	3.03 ± 0.10	1.09 ± 0.1	3068 ± 300	3 ± 1 × 10^{12}	3.77 ± 0.15
$Ru(dmb)_3^{2+}$	3166 ± 418	2 ± 2 × 10^{12}	4.81 ± 0.11	1.33 ± 0.2	2741 ± 622	3 ± 4 × 10^{11}	5.28 ± 0.18
$Ru(dmb)_2(decb)^{2+}$	948 ± 552	2 ± 2 × 10^{7}	10.10 ± 0.46	0.77 ± 0.1	447 ± 140	4 ± 1 × 10^{6}	6.45 ± 1.05
$Ru(dmb)(decb)_2^{2+}$	945 ± 436	2 ± 4 × 10^{7}	5.26 ± 0.45	0.66 ± 0.1	612 ± 134	5 ± 1 × 10^{6}	4.09 ± 0.28
$Ru(decb)_3^{2+}$	2802 ± 152	7 ± 9 × 10^{10}	3.48 ± 0.03	1.34 ± 0.2	1177 ± 514	3 ± 4 × 10^{7}	3.30 ± 0.10

[a] The error margins indicated represent 2σ, from the standard deviations of each point. [b] $[Ru(bpy)_3]^{2+}$ is included with the data for these complexes for comparative purposes. The method of analysis yields $\Delta E'$ and k_0' values somewhat smaller than those reported elsewhere.

Table IV. Room-Temperature Excited-State Decay and Photoanation Parameters

complex	τ, ns	η_{ic} [b]	ϕ_{em}	ϕ_p^{obsd} [a]	ϕ_p^{dd}
$Ru(bpy)_3$	576 ± 0.8	0.84 ± 0.06	0.06 ± 0.01	0.049 ± 0.010	0.57 ± 0.02
$Ru(dmb)_3$	931 ± 25	0.50 ± 0.10	0.12 ± 0.02	0.005 ± 0.002	0.010 ± 0.002
$Ru(dmb)_2(decb)_2$	853 ± 6	0.047 ± 0.02	0.07 ± 0.01	<0.001	
$Ru(dmb)(decb)_2$	1415 ± 9	0.42 ± 0.04	0.10 ± 0.02	<0.001	
$Ru(decb)_3$	2230 ± 56	0.26 ± 0.10	0.30 ± 0.03	0.012 ± 0.005	0.033 ± 0.010

[a] Detection limit of the method is approximately 0.001. [b] Calculated from activation parameters obtained in fit of τ vs. T.

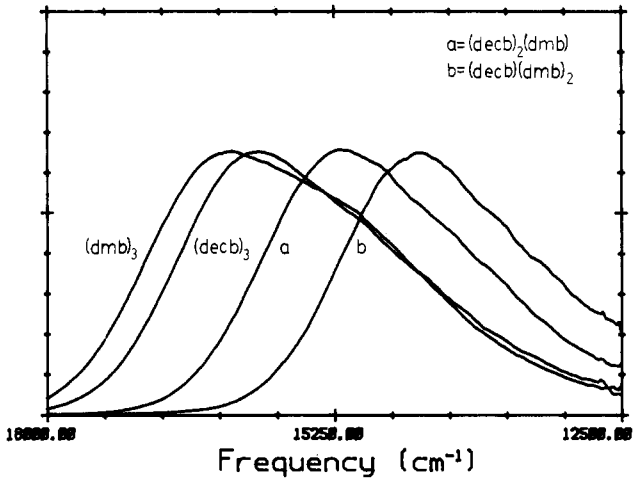

Figure 2. Normalized, corrected emission spectra at room temperature (298 K) in N_2-degassed CH_2Cl_2 for $[Ru(L)_n(L')_{3-n}]$.

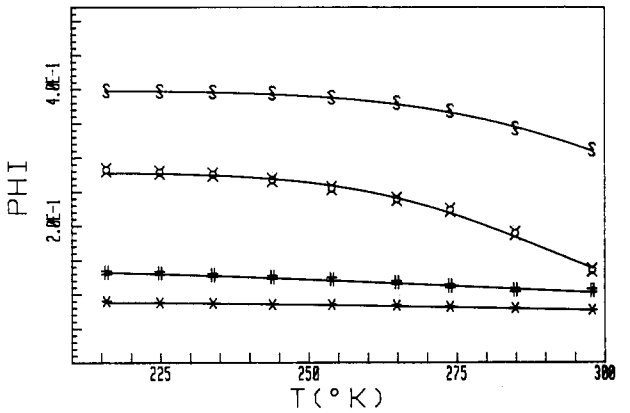

Figure 3. Emission quantum yields for complexes **1**–**4** as a function of temperature for **1** (⊗), **2** (×), **3** (#), and **4** (§). The solid line represents the best fit to the data (see text).

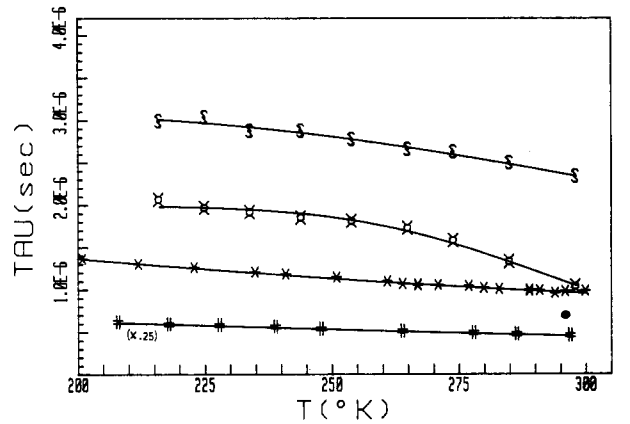

Figure 4. Fits of τ (μs) vs. T (K) in CH_2Cl_2 for **1** (⊗), **2** (×), **3** (#), and **4** (§).

the emitting state is charge transfer in nature[21] and that for **2**, **3**, and **4** emission occurs from the $Ru^{III}(decb)^-$ charge-transfer state.

Temperature Dependence of Emission Quantum Yields and Lifetimes. Corrected luminescence spectra and lifetimes for the complexes were measured as a function of temperature between 220 K and room temperature in methylene chloride. Quantum yields for emission were determined relative to $[Ru(bpy)_3]^{2+}$ at room temperature in water (ϕ_{em} = 0.042 at 298 K).[9b]

Temperature-dependent-emission quantum yield data for each of the complexes is shown in Figure 3. Relative quantum yield measurements were corrected for absorption changes as a function of temperature. **2** and **3** increase by 8%, **1** increases by 12%, and **4** increases by 21% in their molar absorptivities in going from room temperature to 220 K at the excitation wavelength of 450 nm. The most striking temperature-dependent quantum yield effect is that complexes **2** and **3** exhibit a much smaller temperature dependence than **1** or **4**. The data were fit by employing an approach analogous to that initially used by Van Houten and Watts for $[Ru(bpy)_3]^{2+}$ in water[9] and more recently exploited by Meyer[12,13,17] and others[11,14] for spectroscopic characterization of Ru(II) and Os(II) polypyridyl complexes. The temperature-dependent data was fit by employing eq 1, where k_1 represents k_r

$$\phi_{em}^{obsd} = \left[\frac{k_1}{\eta_{isc}k_r} + \frac{k_0'}{\eta_{isc}k_r}\exp(-\Delta E'/RT)\right]^{-1} \quad (1)$$

+ k_{nr}, temperature-independent radiative and nonradiative decay rates, k_0' represents a thermally activated process prefactor with activation energy $\Delta E'$, and η_{isc} represents the quantum efficiency of intersystem crossing to the triplet state. While for $[Ru(bpy)_3]^{2+}$, at temperatures around 77 K, k_{nr} exhibits temperature dependence,[7c] in this work reasonable fits of data measured over a more restricted temperature range were obtained by considering only a single temeprature-dependent parameter. Values of k_1 and k_0' may be obtained since the product $\eta_{isc}k_r$ results from the measured luminescence quantum yield and radiative lifetime at a given temperature:

$$\phi_{em}\tau^{-1} = k_r\eta_{isc} \quad (2)$$

Table III lists values of $\Delta E'$, k_1 and k_0' calculated from fits of ϕ_{em}^{obsd} vs. T. From the results, it is clear that only order of

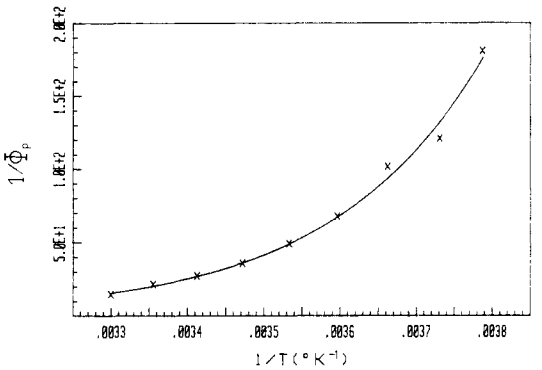

Figure 5. Fit of $(\phi_p^{dd})^{-1}$ vs. $1/T$ (K^{-1}) for photoanation of $[Ru(decb)_3]$ with Cl^- (3×10^{-3} M) in CH_2Cl_2.

magnitude estimates are available for values of k_0', due to the large standard deviation of the fit.

Room-temperature lifetimes are given in Table IV, and the temperature-dependent lifetime data are shown in Figure 4. As with quantum yields, emission lifetimes for **1** and **4** exhibit large increases in τ with decreasing temperatures near room temperature whereas **2** and **3** show only a slight temperature dependence. It is assumed, as in the dependence of ϕ_{em} on T, that there is a single temperature-dependent nonradiative decay pathway (eq 3).

$$\tau = [k_1 + k_0' \exp(-\Delta E'/RT)]^{-1} \quad (3)$$

Figure 4 shows fits obtained for **1–4** and Table III includes values for k_1, and k_0' and $\Delta E'$.

Photoanation by Cl^-. Photolysis of complexes **1** and **4** in N_2-purged methylene chloride containing tetraethylammonium chloride (3.0 mM) by 450 ± 10-nm irradiation results in substitution of bpy by Cl^-. The anation does not depend upon Cl^- concentration between 10^{-5} and 10^{-2} M for the tetraethylammonium salt. Room-temperature values of the observed quantum yield for the photoanation process are listed in Table IV. The most striking feature of the photoreactivity is that complexes **2** and **3** are essentially inert to photoanation at room temperature in dichloromethane. For $[Ru(bpy)_3]^{2+}$, the photoanation yield increases by several orders of magnitude when the dielectric constant of the solvent is decreased.[13] Complexes **2** and **3** exhibit no photolysis products upon monochromatic (450 ± 10 nm) irradiation in acetonitrile or upon 72 h of broad-band photolysis in CH_2Cl_2 containing 3.0 mM chloride with a 150-W Xe arc lamp having a Pyrex UV cutoff filter.

Quantum yields for anation of **1** and **4** employing narrow band excitation (450 ± 10 nm) between 265 and 300 K were measured for nitrogen-purged solutions (Figure 5). The data were fit by assuming that anation occurs only from a ^{3}MC state populated by internal conversion from the ^{3}MLCT state (Scheme I) and that the temperature dependence of the anation, corrected for the temperature dependence of the ^{3}MLCT → ^{3}MC process, results from a thermal barrier to the anation process (eq 4). This

$$(\phi_p^{obsd}/\phi_{ic})^{-1} = (\phi_p^{dd})^{-1} = 1 + k_0'' \exp(\Delta E''/RT) \quad (4)$$

approach has been employed by Durham et al. for anation of $[Ru(bpy)_3]^{2+}$ by SCN^- in CH_2Cl_2.[13] The $\Delta E''$ values obtained for complexes **1** and **4** are 3130 ± 1540 and 3530 ± 334 cm^{-1}, respectively, while that for $[Ru(bpy)_3]^{2+}$ substitution by SCN^- is 1870 cm^{-1}.

Discussion

The complexes examined here have absorption and emission spectra and redox properties similar to those of other tris(bipyridyl) complexes.[1b-e] These complexes all exhibit a single, metal-centered oxidation and three ligand-localized reductions corresponding to sequential reduction of each bipyridine.[22] The absorption spectra have two principal bands with maxima at approximately 300 nm, assigned as an intraligand, $\pi \rightarrow \pi^*$ transition, and between 430 and 500 nm. The longer wavelength absorption maxima in series of related bipyridyl complexes[25-29] are linearly related to the energy

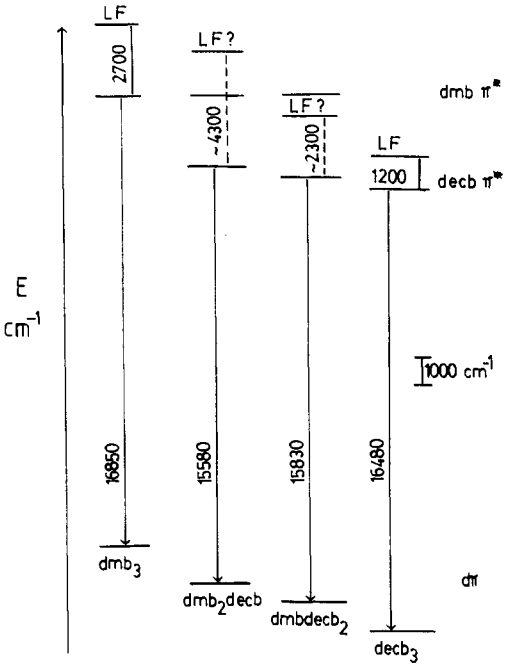

Figure 6. Relative energies of ground and excited states determined from spectroscopic and electrochemical data (see text) and including measured and estimated activation energies (for **2** and **3**) for ^{3}MLCT → ^{3}MC internal conversion.

difference between the first metal-centered oxidation and the first ligand reduction, $\Delta E°$, serving to support assignment of this transition as MLCT in nature. Emission spectra from polypyridyl complexes also exhibit a linear relationship between $\Delta E°$ and emission maxima,[12b,21] and the emitting state has been assigned as a charge-transfer state on the basis of this and other evidence.[6,7] For complexes **1–4**, absorption, emission, and redox properties behave as described above. The $\Delta E°$ values decrease in the order **1** > **4** > **3** > **2**, and both absorption maxima and emission maxima follow the same ordering.

There are several features of the mixed-ligand complexes **2** and **3** of particular interest. The absorption spectra between 400 and 500 nm exhibit two distinct maxima (Figure 1), which may be assigned as d → π^* (decb) and d → π^* (dmb) for the low- and high-energy maxima, respectively. Multiple MLCT maxima have been observed for $[Ru(biq)_2(bpy)]^{2+}$ (biq ≡ 2,2′-biquinoline)[14,24] and for Ru(II) complexes having bipyridine, 2,2′-bipyrimidine and/or 2,2′-bipyrazine.[17] For $[Ru(biq)_2(bpy)]^{2+}$ the d → π^*(biq) maximum occurs at 550 nm, overlapping only slightly with the d → π^*(bpy) transition. The emission spectra of both **2** and **3** have a single maximum between room temperature and 77 K. Emission occurs exclusively from the lowest energy, $d^5\pi^*(decb)^1$, MLCT state (vide infra). No emission is observed from d → π^*(dmb) charge-transfer states. For $[Ru(bpy)_3]^{2+}$, evidence exists from excited-state resonance Raman spectra,[30,36] excitation po-

(25) (a) Callahan, R. W.; Brown, G. M.; Meyer, T. J. *Inorg. Chem.* **1975**, *14*, 1443. (b) Sullivan, B. P.; Salmon, D.; Meyer, T. J.; Pecdrin, J. *Inorg. Chem.* **1979**, *18*, 3369.
(26) Cloninger, K. K.; Callahan, R. W. *Inorg. Chem.* **1981**, *20*, 1611.
(27) Lever, A. B. P.; Licoccia, S.; Magnell, K.; Minor, P. C.; Ramaswamy, B. S. *Adv. Chem. Ser.* **1982**, *No. 201*, 237.
(28) Templeton, J. L. *J. Am. Chem. Soc.* **1979**, *101*, 4906.
(29) Zwickel, A. M.; Creutz, C. *Inorg. Chem.* **1971**, *10*, 2395.
(30) Bradley, P. G.; Kress, N.; Hornberger, B. A.; Dallinger, R. F.; Woodruff, W. H. *J. Am. Chem. Soc.* **1981**, *103*, 7441.
(31) (a) Hipps, K. W. *Inorg. Chem.* **1980**, *19*, 1390. (b) Carlin, C. M.; De Armond, M. K. *Chem. Phys. Lett.* **1982**, *89*, 297.
(32) Morris, D. E.; Hanck, K. W.; DeArmond, M. K. *J. Am. Chem. Soc.* **1983**, *105*, 3032.
(33) Caspar, J. V.; Meyer, T. J. *J. Phys. Chem.* **1983**, *87*, 952.
(34) Wacholtz, W. M.; Auerbach, R. A.; Schmehl, R. H.; Ollino, M.; Cherry, W. R. *Inorg. Chem.* **1985**, *24*, 1758.
(35) Kestner, N. R.; Logan, J.; Jortner, J. *J. Phys. Chem.* **1974**, *78*, 2148.
(36) Caspar, J. V.; Westmoreland, T. D.; Allen, G. H.; Bradley, P. G.; Meyer, T. J.; Woodruff, W. H., submitted for publication.

larization measurements[31] and ESR studies[32] suggesting that the MLCT is localized on a single bipyridine. For **2** and **3** nonradiative relaxation for $d^5\pi^*(dmb)^1$ states to $d^5\pi^*(decb)^1$ states must be rapid relative to radiative decay from the dmb-localized state.

Since the principal interest of this work is the investigation of factors controlling the internal conversion dynamics between the ^{3}MLCT and ^{3}MC states, and presumably the energetic separation between these states, an energy level diagram comparing the various states of **1–4** has been constructed from redox and emission data. Figure 6 demonstrates the relationship between ground $(d\pi)^6$ and excited MLCT $(d\pi)^5(\pi^*(ligand))^1$ states for this series of complexes. The figure is constructed by first choosing an arbitrary energy for the ground state of **1**. The relative ground state energies of the other complexes are then approximated by comparison of the $Ru^{3+/2+}$ potentials, $E°$, for **2–4** to that for **1** (eq 5), where E_{st}

$$E°[\text{decb complex}] - E°[\mathbf{1}] = E_{st} \qquad (5)$$

represents the stabilization of the state relative to **1**. The energy placement of the ^{3}MLCT state relative to the ground state for each complex is then obtained by adding the emission energy to the relative ground-state energy. Ideally, the purely electronic transition energy should be used here; however, the energy of the lowest energy emission maximum at 77 K is employed in this case. Note that this simple procedure results in ^{3}MLCT levels nearly equivalent (varying by 4% of the total emission energy) for the complexes containing decb, as expected where the MLCT^3 is indeed $d^5\pi^*(decb)^1$ in nature for **2–4**. From this diagram, the $d^5\pi^*(dmb)^1$ state lies approximately 4000 cm^{-1} above the $d^5\pi^*$-$(decb)^1$ state. For this series, the relative ordering of absorption and emission energies for **2–4** results from stabilization of the d^6 ground state when the number of decb ligands is increased.

The completion of Figure 6 requires addition of the ^{3}MC states for **1–4**. An upper limit for the ^{3}MC energy is obtained from activation energies determined from quantum yield and lifetime measurements (Table III) provided the activation results in population of the ^{3}MC state. Combination of measured activation energies with photoanation data (Table IV) results in the following observations: (1) complexes **1** and **4** have relatively large $\Delta E'$ values and undergo relatively efficient photoanation at room temperature; (2) **2** and **3** have much smaller activation barriers and are photoinert. Room-temperature values for η_{ic}, the efficiency of internal conversion between ^{3}MLCT and ^{3}MC states (eq 6),

$$\eta_{ic} = \eta_{isc}\left(\frac{k_0' \exp(-\Delta E'/RT)}{k_1 + k_0' \exp(-\Delta E'/RT)}\right) \qquad (6)$$

given in Table IV, are relatively high for all the compounds reported. If η_{ic} represents crossover to a ^{3}MC state, then changes in η_{ic} should reflect generally on the efficiency of anation. For **1** and **4** the quantum yield for photoanation decreases as the temperature is lowered (and η_{ic} decreases) as required if anation occurs from the thermally accessed state. Thus the activation barriers may be included in Figure 6 as barriers to population of ^{3}MC states, analogous to those in $[Ru(bpy)_3]^{2+}$.[9,13]

The observed anation efficiencies for **2** and **3** are too small to measure and do not agree with this approach. This discrepancy can be reconciled in three possible ways: (1) the anation activation energy from the ^{3}MC state is much larger for the mixed ligand complexes; (2) the low activation energies for the mixed complexes do not represent ^{3}MLCT to ^{3}MC interconversion; (3) the activated nonradiative pathway for the ^{3}MLCT has nothing to do with photoanation. Of the three statements, (2) is considered to be the most likely. While (1) may contribute to the low photoanation, it is not clear why the mixed complexes should have anation activation energies greatly different from those of the tris complexes. Finally, while (3) is always a possibility, it does not need to be invoked given other satisfactory explanations. It seems inherently reasonable that the ^{3}MC state is the photolabile pathway given its electronic configuration and its probable energy position in the state manifold. The remaining discussion focuses on (a) explaining the origin of the observed activation barriers for **2** and **3** and (b) exploiting existing information to obtain an estimate for the ^{3}MLCT → ^{3}MC activation barrier for **2** and **3**.

Given that the low activation barriers for the mixed complexes do not represent ^{3}MLCT → ^{3}MC transitions, an explanation for an activation barrier of this magnitude is required. Others observing similar phenomena in mixed-ligand ruthenium(II) bipyridyl complexes have offered the following explanations.

(I) The activated process represents population of a MLCT state principally singlet in character.[37,17] A recent modeling of the excited state of $[Ru(bpy)_3]^{2+}$, assuming a localized excited state and including spin–orbit coupling,[37] predicts such a state approximately 600 cm^{-1} above the manifold of three ^{3}MLCT states that have been experimentally observed. Variable-temperature polarized single-crystal emission spectra of $[Ru(bpy)_3]^{2+}$ indicate the presence of a weak emission of higher energy (650 cm^{-1}).[38] For the mixed-ligand complexes here, attempts to observe a rapid emission decay from the activated state at room temperature have been unsuccessful.

(II) Because of the symmetry lowering from D_3 to C_2 in the mixed-ligand complexes, the ^{3}MLCT state may be split into two different $d^5\pi^{*1}$ states in which the electronic configuration in the d levels differ. Emission could occur from each of these states, in thermal equilibrium with one another.[14] This case also suggests blue shift in emission as the temperature is increased. Here, the lifetime should be dominated by the fact that the emitting state is ^{3}MLCT, and lifetimes for emission of the two states should be comparable. Assuming the activated nonradiative decay process does correspond to population of the higher energy MLCT state, the prefactor for the decay, k_0', represents the nonradiative decay rate from the higher energy state. For mixed-ligand complexes observed,[11,14,17] values of k_0' vary from 6×10^6 to 3×10^7 s^{-1}; the rates are larger than k_{nr}^0 for the temperature-independent emission, but are not so fast that the state-splitting argument may be discounted.

(III) Since the emission maximum varies with temperature, it is possible that k_{nr} also exhibits temperature dependence. The magnitude of the effect can be assessed by fitting of emission spectra at a variety of temperatures. Although such analyses have not been performed, the feasibility of the argument has been demonstrated.[17]

The activation energies for ^{3}MLCT → ^{3}MC internal conversion for **2** and **3** can be approximated from information available. To see this, a more detailed account of the activated nonradiative decay of **1** and **4** is necessary. Employing Scheme I results in the steady-state emission quantum yield for the ^{3}MLCT being given by

$$\phi_{em} = k_r/(k_1 + k(T)) \qquad k(T) = (k_2k_3)/(k_{-2} + k_3) \qquad (7)$$

where k_r is the radiative rate of the ^{3}CT state ($k_1 = k_r + k_{nr}$). The temprature dependence of the quantum yield then comes about from the term $k_2k_3/(k_{-2} + k_3)$ since both k_2 and k_{-2} have a temperature-dependent activation behavior.

Assuming that decay of the ^{3}MC state is rapid relative to relaxation of the ^{3}CT state, dynamic analysis of an initial population of excited ^{3}CT states, C_0, results in the expression (see Appendix I)

$$^3\text{CT} \cong C_0 \exp[-(k_1 + k(T))t] \qquad (8)$$

As in the steady-state quantum yield, the temperature-dependent component to the lifetime comes about from the same term $k(T)$ within the limiting case stated above. Two limiting cases for $k(T)$ can be imagined.

(1) $k_3 >> k_{-2}$: In this case $K(T) = k_2$. The temperature-dependent term is the forward electron-transfer rate, and the activation energy is given by eq 9. The term E represents the

(37) (a) Kober, E. M.; Meyer, T. J. *Inorg. Chem.* **1984**, *23*, 3877. (b) Kober, E. M.; Meyer, T. J. *Inorg. Chem.* **1983**, *22*, 1614.
(38) Yersin, H.; Gallhuber, E.; Vogler, A.; Kunkely, H. *J. Am. Chem. Soc.* **1983**, *105*, 4155–6.
(39) (a) Braterman, P. S.; Harriman, A.; Hearth, G. A.; Yellowlees, L. J. *J. Chem. Soc., Dalton Trans.* **1983**, 1801. (b) Creutz, C.; Sutin, N. *Adv. Chem. Ser.* **1978**, *No. 168*, 1.

$$k_2 = k_2^0 \exp(-\Delta E'/RT) \qquad \Delta E' = (\chi + E)^2/4\chi$$
$$k_2^0 = (2\pi V^2/h)(1/4\pi\chi RT)^{1/2} \tag{9}$$

internal energy change occurring upon electron transfer, V is the electronic coupling matrix element between ^{3}MLCT and ^{3}MC, and $\chi/4$ is the classical vibrational trapping frequency.[1c]

(2) $k_{-2} >> k_3$: Here $K(T) = (k_2/k_{-2})k_3$. This equilibrium limit has as its activation energy, E, the difference in energy between the ^{3}CT and ^{3}MC levels. The prefactor for the activated process is then $(k_2^0/k_{-2}^0)k_3$ (with the superscript referring to individual electron-transfer prefactors of eq 9). It is a priori not possible to distinguish these cases.

For complexes **2** and **3**, the activation energy for the population of the ^{3}MC state or the energetic separation between the ^{3}MLCT and ^{3}MC states can be approximated by assuming that **1**–**4** exhibit emission that strictly follows either case 1 or case 2 above. In the equilibrium limit, case 2, the measured activation energy represents the energetic separation between the charge-transfer and metal-centered states. The energy of the ligand field transition, to populate the ^{3}MC state, can be approximated by the sum of the emission energy and the activation barrier from lifetime measurements. For complexes **1** and **4**, the energies are 19 600 and 17 700 cm^{-1}, respectively. The ^{3}MLCT – ^{3}MC energetic separation for **2** and **3** may be approximated by assuming that the ligand field transition energies reflect an environment representing fractional contributions from dmb and decb ligands.[40] Thus for **2**, the ligand field state should be 19 000 cm^{-1} above the ground state and the ^{3}MLCT to ^{3}MC separation is approximately 3420 cm^{-1}. For complex **3**, the average ligand field approach yields a separation of only 2500 cm^{-1} between the charge-transfer and metal-centered states. An important factor to consider in relating photoanation to population of the ^{3}MC state is the internal conversion efficiency, η_{ic}, which depends upon the prefactor to the temperature-dependent decay as well as the energetic separation between ^{3}MLCT and ^{3}MC states (eq 6). In the equilibrium limit, k_0' corresponds to $(k_2^0/k_{-2}^0)k_3$; assuming that this prefactor for **2** and **3** is approximately the same as that for **4**, η_{ic} may be determined by using the activation barriers determined from the average ligand field approach above. For both complexes η_{ic} is much smaller than that for either **1** or **4**, being approximately 3×10^{-6} and 4×10^{-4} for **2** and **3** respectively. Even if the estimated prefactor is a factor of 10 low, the η_{ic} calculated with the higher k_0' is still small relative to η_{ic} for **1** and **4** (Table IV).

Activation barriers for the ^{3}MLCT → ^{3}MC internal conversion for **2** and **3** may also be estimated when the predominant rate-determining step for internal conversion is k_2 ($k_3 >> k_{-2}$, case 1). In this case the rate k_2 and its activation energy are given by eq 9, given that the ^{3}MLCT to ^{3}MC transition corresponds to a "normal-region" electron transfer.[1c,12,33,35] In order to discuss comparative cases, the assumption is made that χ is about the same for all molecules (within a factor of 2). Such an assumption is reasonable since coordinates involved in electron transfer will be the same for all compounds. The mixed-complex activation energies may be written in terms of the energy of **4** as (see Appendix II)

$$\Delta E_3' = 1.3\Delta E_4' + \frac{2.28(E_4 + \chi)}{4\chi}\epsilon_3 + \epsilon_3^2/4\chi$$
$$\Delta E_2' = 1.64\Delta E_4' + \frac{2.56(E_4 + \chi)}{4\chi}\epsilon_2 + \epsilon_2^2/4\chi \tag{10}$$

Although the values of χ, E_4, $\Delta E_3'$, and $\Delta E_2'$ cannot be independently determined, all values may be determined as a function of χ by employing eq 10 and eq 9 and are given in Table V. It is clear that for reasonable values of χ, activation energies of the mixed complexes are large. Use of $\Delta E_3'$ to calculate ϕ_{ic}, once again assuming k_0' is approximately the same as that for **4**, demonstrates that no thermally activated contribution to the nonradiative rate is expected at room temperature or below (Table V). The model of eq 10 as presented limits χ to be no greater than ~5000 cm^{-1}, at which time it predicts a reversal of level ordering of the ^{3}MC and ^{3}MLCT states. Since state reversal would create easily observable changes in emission, it is clear that this does not occur. The exact numerical placement of such a boundary on χ should, however, be viewed by considering the initial approximations chosen (such as χ is the same for all complexes). Several meaningful observations do result from the approximation. First, $\Delta E_2' > \Delta E_3'$, and second, for all reasonable choices of parameters it can be expected that all activation energy barriers are on the order of 2000 cm^{-1} or greater.

Table V. Estimates of $\Delta E'$ for Mixed Complexes for Several Values of χ[a]

χ	E_4	E_3	E_2	E_1	$\Delta E_3'$	$\Delta E_2'$	$\phi_{ic,3}$[b]
5000	−148	1295	3586	2404	1981	3686	0.006
2000	1068	2198	4177	2683	2202	4769	0.002
1000	1169	2141	3963	2311	2466	6157	0.0006
500	1034	1895	3605	1841	2868	8425	0.0001

[a] All E, E', and χ values in cm^{-1}. $\Delta E_1'$ and $\Delta E_4'$ taken from Table III for τ vs. T data; $\epsilon_2 = 2033$ cm^{-1}, and $\epsilon_3 = 592$ cm^{-1}. [b] Calculated from eq 8, assuming $k_0' = 3.4 \times 10^7$ and $\eta_{isc} = 1.0$.

Thus in either of the two limiting cases, the activation energies observed for **2** and **3** are consistent with the presumed kinetic scheme proposed to account for photoanation and are arguably high enough to account for the lack of photoanation.

Another item of a more speculative nature should be discussed within the model presented. The change in k_0' between **1** and **4** is approximately a factor of 10^4. This may reflect that case 2, the equilibrium limit, may in fact be important at least for **4**. It seems difficult to envision how changes in χ, V, and entropic factors can account for such a large change in k_0' between **1** and **4**, which would be necessary for case 1. In contrast, a ratio of constants making up k_0' in case 2 is easier to rationalize having a 10^4 change between these compounds.

Emission Quantum Yields and Lifetimes. The temperature dependence of luminescence quantum yields and lifetimes of **1**–**4** allows determination of activation parameters for nonradiative decay by employing eq 1 and eq 2. Data obtained from fits of ϕ_{em} vs. T and τ vs. T are listed in Table III. For the complexes containing decb ligands, significant differences exist for $\Delta E'$ values determined by the two independent methods. Determination of emission quantum yields present difficulties that significantly lower the precision of the experiment, such as correction for photomultiplier tube response, absorbance matching for relative quantum yield measurements, and correction for variations in absorbance with temperature. However, within the limitations of precision, the parameters obtained in the best fits of τ and ϕ_{em} vs. T were employed to calculate $k_r\eta_{isc}$ as a function of T (eq 11).

$$k_r^T\eta_{isc} = (\phi_{em}^T)(\tau^T)^{-1} \tag{11}$$

Plots of k_r vs. T provide a test of the above assumptions made concerning the constancy of η_{isc} and k_r on fits of ϕ_{em} with T. It is expected that k_r will be nearly invariant with temperature. For the mixed-ligand complexes examined, **2** and **3**, the calculated $k_r\eta_{isc}$ values vary by less than 5% over the entire temperature range studied. Complexes **1** and **4** exhibit about a 20% decrease in $k_r\eta_{isc}$ as the temperature is raised from 180 to 300 K. Variations in $k_r\eta_{isc}$ with temperature suggest that η_{isc} may be somewhat less than unity at room temperature. Recently, other modified bipyridyl complexes have been examined that demonstrate temperature-dependent η_{isc}.[34]

Summary

The photophysical and photochemical properties of mixed-ligand polypyridyl ruthenium(II) complexes **1**–**4** demonstrate that the energetic separation between the substitution-inert ^{3}MLCT state

(40) Figgis, B. N. "Introduction to Ligand Fields"; Interscience: New York, 1966; p 236.
(41) Maerker, G.; Case, F. H. *J. Am. Chem. Soc.* **1958**, *80*, 2745.
(42) Sawyer, D. T.; Roberts, J. L. "Experimental Electrochemistry for Chemists"; Wiley-Interscience: New York, 1974; p 212.
(43) Hatchard, C. G.; Parker, C. A. *Proc. R. Soc. London, Ser. A* **1956**, *235*, 51.
(44) Marquardt, D. W. *J. Soc. Ind. Appl. Math.* **1963**, *11*, 431.

Table VI. Analytical Data for the Complexes Examined[a]

complex	% C		% H		% N	
	calcd	found	calcd	found	calcd	found
$[Ru(dmb)_3]$	45.61	45.80	4.07	3.85	8.70	8.91
$[Ru(dmb)_2(decb)]$	45.19	45.31	3.94	3.81	7.97	7.93
$[Ru(dmb)(decb)_2]$	44.65	44.92	3.98	3.77	7.44	7.14
$[Ru(decb)_3]$	44.72	44.38	3.90	3.72	6.53	6.51

[a] Analyses are for the PF_6 salts as anhydrous powders.

and the reactive ^3MC state may be controlled by designing complexes having a ligand with a low-energy π^* level and several ligands that serve as good σ donors and π acceptors. The mixed-ligand complexes **2** and **3** are inert to photosubstitution and exhibit very small activation barriers to nonradiative deactivation; the activated decay certainly does not involve population of a ^3MC state and may be rationally explained as population of an MLCT state having a large degree of singlet character. Predictions of $\Delta E'$ for the $^3MLCT \rightarrow {}^3MC$ process based upon an average ligand field approach or from estimates of values of χ, result in estimates of ϕ_{ic} that are $\leq 10^{-3}$ at room temperature for **2** and **3**. The calculations predict that **2** should be exceptionally stable with respect to photoanation. Very recently we have prepared complexes of the general type $[Ru(decb)_{1-2}(dmb)_{1-0}(py)_2]^{2+}$; unlike the majority of bis(pyridine)ruthenium(II) complexes, these exhibit strong emission at room temperature, as expected on the basis of an average ligand field approach applied to these systems to estimate energies of ^3MC states. Complete photophysical and photochemical examination of these bis(pyridine) complexes is currently in progress.

Experimental Section

Materials. 4,4′-Dicarboxy-2,2′-bipyridine was synthesized by literature methods.[45] $[Ru(bpy)_3]^{2+}$, **1**, and **4** were prepared by using modifications of literature procedures[45] with ethanol used as solvent in place of DMF, and the PF_6^- salts were precipitated by the addition of saturated aqueous NH_4PF_6. All complexes were purified by chromatography on Alcoa type F-20 alumina employing toluene/acetonitrile mixtures as eluent. Microanalytical data (Gailbraith Laboratories, Knoxville, TN) for the complexes are given in Table VI.

Acetonitrile for electrochemical measurements (Burdick and Jackson) was refluxed over CaH_2 and distilled immediately prior to use. Dichloromethane (Aldrich, spectrophotometric grade) was used without further purification.

Preparations. **$[Ru(dmb)_2(decb)](PF_6)_2$.** $[Ru(dmb)_2Cl_2 \cdot 2H_2O]$[45a] (0.5 g, 0.868 mmol) and 4,4′-bis(ethylcarboxy)-2,2′-bipyridine (0.261 g, 0.868 mmol) were heated at reflux in ethanol (50 mL) for 3 h. The ethanol was removed by evaporation, and the remaining solid was taken up in water (50 mL). The complex was precipitated with aqueous ammonium hexafluorophosphate and collected by vacuum filtration. The crude material was separated from unreacted starting materials by column chromatography on alumina using 1:1 acetonitrile/toluene as eluent. UV–vis, nm (ϵ, M^{-1} cm^{-1}): 430 (12 400), 492 (13 020). IR: ν_{CO} = 1730 ± 5 cm^{-1}.

$[Ru(dmb)(decb)_2](PF_6)_2$. $[Ru(decb)_2Cl_2]$[45a] (0.5 g, 0.643 mmol) and 4,4′-dimethyl-2,2′-bipyridine (0.118 g, 0.643 mmol) were heated at reflux in ethanol (50 mL) for 6 h. The reaction mixture was worked up and purified chromatographically as above. Since the decb ligand undergoes slow hydrolysis on alumina, the chromatography is performed as rapidly as possible to minimize loss of complex. The hydrolyzed complex binds irreversibly to the column. UV–vis, nm (ϵ, M^{-1} cm^{-1}): 370 (14 500), 442 (14 590), 484 (16 280). IR: ν_{CO} = 1730 ± 5 cm^{-1}.

Equipment. Absorption spectra in methylene chloride solution were obtained by using a Hewlett-Packard 8451A diode array spectrophotometer. Infrared spectra were obtained as KBr pellets or mulls on NaCl plates and were recorded on a Perkin-Elmer Model 683 spectrophotometer. Fluorescence spectra were obtained by using a Spex Industries Model 111C fluorescence spectrometer equipped with a 450-W Xe arc lamp and cooled PMT housing. Emission spectra were corrected for photomultiplier falloff to 850 nm.

Emission Quantum Yields. Room-temperature emission quantum yields were measured for nitrogen-purged solutions of each complex in quartz cuvettes. Emission measurements were made at 90° relative to excitation and were corrected for lamp fluctuation and photomultiplier response. Quantum yields for complexes **1–4** were calculated from the integrated emission spectra relative to $[Ru(bpy)_3]^{2+}$ in water (ϕ_r = 0.042 at 298 K)[9b] and corrected for refractive index differences between H_2O and CH_2Cl_2 by employing the relationship

$$\phi_r = \phi_r^{obsd}(\eta/\eta_{H_2O})^2$$

where ϕ_r^{obsd} is the uncorrected emission quantum yield and η is the refractive index of CH_2Cl_2. Excitation of all solutions, absorbance matched at 0.2 ODU, was at 450 nm.

Temperature-dependent quantum yield measurements were made by using an Oxford Instruments DN 1704 liquid-nitrogen cryostate thermostated by a DTC-2 Digital temperature controller using a Pt resistance thermometer attached to the heat-exchange block of the cryostat. An independent Pt thermistor attached to the sample cell was employed for temperature measurement. Sample cells for variable-temperature work consisted of vacuum-sealed 12-mm Pyrex test tubes containing freeze–pump–thaw degassed samples. Solutions were prepared such that the absorbance was ≤0.20. In experiments using test tubes, measurements were made without altering the position of the tube in the apparatus. Low-temperature quantum yields, corrected for increases in solution absorbance (≈10% at 220 K), were determined relative to the room-temperature emission of the sample.

Photochemistry. Quantum yields for photoanation were measured by monitoring the decay of the emission as a function of time using irradiation from the previously described fluorimeter. The procedure involved mixing equal volumes of CH_2Cl_2 solutions of tetraethylammonium chloride (6.2×10^{-3} M) and the complex ($\cong 10^{-5}$ M) in a 1-cm fluorometric cell in the dark. The solutions were N_2 bubble degassed for 30 min prior to irradiation, and a blanket of CH_2Cl_2-saturated N_2 was passed over solutions during irradiation. The decrease in complex emission intensity, measured at right angles to excitation, was monitored as a function of time of irradiation. Quantum yields were determined at times representing less than 10% conversion to product. Ferrioxalate actinometry[41] was performed in the same cell under indentical conditions.

Lifetimes. Lifetime measurements were obtained with a PRA Model LN100 Nitromite nitrogen laser (350 ps pulse width) as excitation source. The samples were freeze–pump–thaw degassed (5–6 cycles) and mounted in the Oxford Instruments Dewar described above for all measurements at room temperature and below. The laser pulse was passed through a Schott UG-11 colored glass filter and focused to approximately 1-mm diameter on the sample. Emitted light was collected at 90° from the incident excitation beam, filtered with a Schott GG-375 colored glass filter, and imaged onto the entrance slit of a GCA/McPerson EU-700 monochromator. The line of excitation through the sample was rotated 90° during imaging with a dove prism. The improvement in filling the monochromator slit via this arrangement provided a factor of 5 increase in signal. The emitted light was detected with a Hammamatsu R777 PMT in a Pacific Instruments 3150RF holder. Time behavior of the emission intensity was monitored with a PAR 162 boxcar with a PAR 166 gated integrator plug-in. Triggering was accomplished by splitting off a fraction of a laser beam to saturate a 1P28 photomultiplier tube. The boxcar aperature duration was always 50 ns or less, and the observed time constant was always one laser pulse or less. Experiments were controlled by a Hewlett-Packard 9826 microcomputer interfaced to a HP 6940B multiprogrammer.

Lifetime data were analyzed by using a nonlinear least-squares fit to exponential decay with a baseline (vide infra). The fitting program uses a modified Marquardt algorithm for least squares minimizations.[44]

Electrochemical Measurements. Cyclic voltammetry was performed by employing an EG&G, Princeton Applied Research Model 173 potentiostat equipped with a Model 176 current follower and a Model 175 universal programmer. Voltammograms were recorded on a Hewlett-Packard Model 7015B X-Y recorder. Measurements were made by using two-compartment cell employing a Pt-disk working electrode (0.15 cm^2) and a Pt-ring counter electrode in one compartment with the reference, SSCE, in the second compartment, linked through a medium-porosity sintered-glass disk to the working electrode compartment. All voltammograms were recorded in acetonitrile solutions having tetrabutylammonium hexafluorophosphate as supporting electrolyte.

Acknowledgment. The authors thank Dr. T. J. Meyer for several helpful discussions and several preprints. Acknowledgement is made to the donors of the Petroleum Research Foundation (R.H.S. and R.A.A.), administered by the American Chemical Society, and to the Research Corp. for partial support of this work.

Appendix I

The time decay of an initial population, C_0, is given by

(45) (a) Sprintschnik, G. H. W.; Kirsch, P. P.; Whitten, D. G. *J. Am. Chem. Soc.* **1977**, *99*, 4947. (b) Gaines, G. L.; Behnken, P. E.; Valenty, S. J. *J. Am. Chem. Soc.* **1978**, *100*, 6549.

$$[^3CT] = C_0/(\lambda_1 - \lambda_2)[(\lambda_2 - k_d)\exp(-\lambda_2 t) + (k_d - \lambda_1)\exp(-\lambda_1 t)]$$

$$\lambda_2 = [(k_c + k_d) + [(k_c + k_d)^2 + 4k_2k_{-2}]^{1/2}/2] > 0$$

$$\lambda_1 = [(k_c + k_d) - [(k_c + k_d)^2 + 4k_2k_{-2}]^{1/2}/2] > 0 \quad (12)$$

$$k_d - \lambda_1 > 0 \qquad k_d = k_{-2} + k_3$$

$$\lambda_2 - k_d > 0 \qquad k_c = k_1 + k_2$$

In the general case, the molecules decay with a biexponential decay. One rate reflects the extra pathway of initial population of the ^{3}MC state before significant electron back-transfer occurs. The other rate reflects the equilibrium decay of the system. A significant simplification can be made if it is assumed that $k_d >> k_c$. This is a reasonable assumption given that (1) clear experimental evidence for the ^{3}MC state has not been demonstrated for $[Ru(bpy)_3]^{2+}$ via techniques such as flash photolysis,[39] indicating k_3 must at least be larger and possibly much larger than k_1 and that (2) the electron-back-transfer rate, k_{-2}, should be larger than the forward, k_2, since the reaction coordinate is the same and the transfer is now exothermic. For $k_d >> k_c$

$$^3CT \cong C_0[(k_d + \gamma - k_c)/(k_d + 2\gamma - k_c)]\exp[-(k_1 + k(T))t] + C_0[\gamma/(k_d + 2\gamma - k_c)]\exp[-(k_d + \gamma)t] \quad (13)$$

$$\gamma = k_2k_{-2}/k_d$$

Since k_d is very large on the emission time scale, this reduces to eq 8.

Appendix II

An expression for the activation energies of **2** and **3** may be obtained from the known activation energies of **1** and **4** and the emission energies of all the complexes. Since the activation energies of **1** and **4** are known, the ratio gives a relation for E_1, E_4, and χ:

$$E_1 = 1.53E_4 + 0.53\chi \quad (14)$$

The energy differences for the mixed-ligand complexes, E_3 and E_2, may be expressed in terms of the emission energies, E_{em}, and the energy differences E_1 and E_4:

$$E_2 = \epsilon_2 + \tfrac{2}{3}E_1 + \tfrac{1}{3}E_4 \qquad E_3 = \epsilon_3 + \tfrac{1}{3}E_1 + \tfrac{2}{3}E_4$$

$$\epsilon_2 = \tfrac{2}{3}E_{em,1} + \tfrac{1}{3}E_{em,4} - E_{em,2} \quad (15)$$

$$\epsilon_3 = \tfrac{1}{3}E_{em,1} + \tfrac{2}{3}E_{em,4} - E_{em,3}$$

These are the same expressions as in the equilibrium case except that the correspondence of the energy difference between excited states and the activation energy is no longer justified. The mixed-complex activation energies may then be written in terms of the energy of **4** by employing eq 9, 14, and 15, which yields eq 10 (see text).

Registry No. $[Ru(dmb)_3](PF_6)_2$, 83605-44-1; $[Ru(dmb)_2(decb)](PF_6)_2$, 99617-91-1; $[Ru(dmb)(decb)_2](PF_6)_2$, 96897-29-9; $[Ru(decb)_3](PF_6)_2$, 75324-94-6; $[Ru(dmb)_3]^{3+}$, 47837-95-6; $[Ru(dmb)_2(decb)]^{3+}$, 99617-92-2; $[Ru(dmb)(decb)_2]^{3+}$, 96897-36-8; $[Ru(decb)_3]^{3+}$, 83605-72-5; $[Ru(dmb)_3]^{+}$, 65605-26-7; $[Ru(dmb)_2(decb)]^{+}$, 99617-93-3; $[Ru(dmb)(decb)_2]^{+}$, 96897-55-1; $[Ru(decb)_3]^{+}$, 83605-73-6; $Ru(dmb)_3$, 83605-52-1; $Ru(dmb)_2(decb)$, 99617-94-4; $Ru(dmb)(decb)_2$, 96897-62-0; $Ru(decb)_3$, 83605-74-7; $[Ru(dmb)_3]^{-}$, 83605-53-2; $[Ru(dmb)_2(decb)]^{-}$, 99617-95-5; $[Ru(dmb)(decb)_2]^{-}$, 96897-69-7; $[Ru(decb)_3]^{-}$, 83605-75-8; $Ru(dmb)_2Cl_2$, 68510-55-4; $Ru(decb)_2Cl_2$, 70281-20-8.

Contribution from the Chemistry Department, University of British Columbia, Vancouver, British Columbia, Canada V6T 1Y6

Trichloro-Bridged Diruthenium(II,III) Complexes: Preparation, Properties, and X-ray Structure of $Ru_2Cl_5(chiraphos)_2$ (chiraphos = 2(*S*),3(*S*)-Bis(diphenylphosphino)butane)

Ian S. Thorburn, Steven J. Rettig,[1] and Brian R. James*

Received June 7, 1985

The triply chloro-bridged, formally mixed-valence compounds $[RuCl(P\text{-}P)]_2(\mu\text{-}Cl)_3$ have been prepared by phosphine exchange from Ru(III) precursors containing PPh_3 or P(*p*-tolyl)$_3$ (P-P: chiraphos, 2(*S*),3(*S*)-bis(diphenylphosphino)butane; $PPh_2(CH_2)_nPPh_2$, n = 3 or 4; diop, 4(*S*),5(*S*)-bis((diphenylphosphino)methyl)-2,2-dimethyl-1,3-dioxolane). The chiraphos complex **1** has been characterized by X-ray analysis and is a highly symmetrical $(\mu\text{-}Cl)_3$ species with irregular octahedral geometry about each Ru (space group *P*1; a = 11.826 (2) Å, b = 11.968 (1) Å, c = 12.075 (2) Å, α = 112.333 (6)°, β = 92.409 (9)°, γ = 103.006 (7)°; Z = 1; the structure was refined to a conventional R value of 0.035 by using 6782 significant reflections and 405 variables). The crystallography data for **1**, and near-infrared spectral data in a range of solvents, show the dimers to be valence-delocalized. The complexes undergo disproportionation rapidly in CH_3CN and more slowly in Me_2SO and CH_3NO_2 to give dimeric Ru^{III}_2 and Ru^{II}_2 species. In CCl_4 or toluene, **1** exists in some other valence-delocalized form, possibly as a tetranuclear cluster.

Introduction

Previous work from this laboratory has described the use of $RuHCl(diop)_2$ as a catalyst for asymmetric hydrogenation (diop = 4(*S*),5(*S*)-bis((diphenylphosphino)methyl)-2,2-dimethyl-1,3-dioxolane).[2,3] Mechanistic studies revealed that the active species contained one diop per Ru(II) center, and this led us to investigate pathways to synthesize complexes containing Ru^{II}(P-P) moieties, where P-P is a chelating bis(tertiary phosphine) such as diop, chiraphos (2(*S*),3(*S*)-diphenylphosphino)butane), or a nonchiral analogue $PPh_2(CH_2)_nPPh_2$, where n = 4 (dppb), 3 (dppp), or 2 (dppe). Such catalysts would be analogous to the well-studied Rh^{I}(P-P) systems.[4-6] The complexes containing monodentate tertiary phosphines, $[RuCl_2(PR_3)_2]_2$, can be conveniently made by reduction of ruthenium(III) precursors such as $RuCl_3(PR_3)_2$,[7,8]

(1) Experimental Officer, University of British Columbia Crystal Structure Service.
(2) James, B. R.; McMillan, R. S.; Morris, R. H.; Wang, D. K. W. *Adv. Chem. Ser.* **1978**, *No. 167*, 122.
(3) James, B. R.; Wang, D. K. W. *Can. J. Chem.* **1980**, *58*, 245.
(4) Kagan, H. B. "Comprehensive Organometallic Chemistry"; Wilkinson, G., Ed.; Pergamon: Oxford, 1982; Vol. 8, p 463.
(5) Halpern, J. *Pure Appl. Chem.* **1983**, *55*, 99.
(6) Bakos, J.; Tóth, I.; Heil, B.; Markó, L. *J. Organomet. Chem.* **1985**, *279*, 23.
(7) James. B. R.; Thompson, L. K.; Wang, D. K. W. *Inorg. Chim. Acta* **1978**, *29*, L237.
(8) Dekleva, T. W.; Thorburn, I. S.; James, B. R. *Inorg. Chem. Acta* **1985**, *100*, 49.

0020-1669/86/1325-0234$01.50/0